대한기계학회 2000년도 추계학술대회논문집 B pp. 142~149 KSME 00F138

산업용 가스터빈 연소기에 대한 실험적 연구

안토노브스키*· 안국영*

EXPERIMENTAL STUDY ON THE HEAVY-DUTY GAS TURBINE COMBUSTOR

V. Antonovsky*, Kook-Young Ahn*

Key Words: Liner Wall Temperature(라이너벽면온도), Combustion Efficiency(연소효율), Pattern Factor(패턴인자), Pressure Loss Factor(압력손실인자), Flame Radiation(화염복사), NOx(질소산화물)

Abstract

The results of stand and field testing of a combustion chamber for a heavy-duty 150 MW gas turbine are discussed. The model represented one of 14 identical segments of a tubular multican combustor constructed in the scale 1:1. The model experiments were executed at a pressure smaller than in the real gas turbine. The combustion efficiency, pressure loss factor, pattern factor, liner wall temperature, flame radiation, fluctuating pressure, and NOx emission were measured at partial and full load for both model and on-site testing. The comparison of these items of information, received on similar modes in the stand and field tests, has allowed the development of a method of calculation and the improvement of gas turbine combustors.

1. INTRODUCTION

Before manufacturing and field testing of the subject combustor for a 150 MW heavy-duty gas turbine, a model testing of the combustor was carried out on a special large-scale stand. The model combustor represented the final variant of the combustion chamber, which had been as a result of numerous experiments, provided with different liners, burners and atomizers, as well as dilution devices. We have made assumptions in the presentation of the results of the comparative experiments at stand and on-site operating conditions. It is completely clear, that the opportunity to compare model and real parameters of the combustion chamber provides a good possibility to improve the method of design and calculation of gas turbine combustors.

* 한국기계연구원

2. COMBUSTION CHAMBER. MODEL AND FIELD TEST PROGRAM

The heavy duty gas turbine GTE-150 was designed according to a simple thermal circuit with one shaft turbogroup and was intended for both peak load and semi-peak load operation. According to this concept, the combustion chamber was constructed as a tubular (multican) type. Fourteen identical liners were placed in separate sections, the axes of which were parallel to the axis of the turbogroup. A section of the combustor is illustrated in Fig. 1a. In addition to the liner, each section contains an atomizer, a vane swirler, a pressure casing, a burner device and a transition piece. Between sections, the connecting branch pipes are established, inside of which interconnectors are located. In this way the problem of pressure alignment between next sections, as well as the

light-round problem was solved. The compressed air enters the volume of the connecting cylinder and is distributed between the sections of the combustor. About 25 % of the air enters the four dilution holes. The remainder of the air passes into the annular channels between casings and liners. On its way to the burner devices, the air is allocated to cooling and combustion holes. The high-speed jets of air leaving the combustion holes provide a rather productive fuel-air mixing that contribute to intensive burning of the fuel and makes possible the light-round of the sections. A vane air swirler with a vane outlet angle of 45° is used as a flame stabilizer. The transition piece connects the liner with the turbine vanes. The combustor of GTE-150 has a combustion loading rate U_S = 174.9 W/m^2/Pa, the combustion product temperature at the exit of the transition piece t_{1T} = 950℃, Combustor inlet air temperature t_A = 372℃, combustor inlet air pressure PA = 1.29MPa.

In this paper the results of testing of the combustion chamber with single burner device are presented. The results of a testing of a combustor with a five-burner device, as shown in Fig. 1b, were published earlier [1].

In the gas turbine GTE-150, air-assist atomizers were used. In these atomizers, a high quality atomization has been achieved. This has been done with a combination of pressure-swirl atomization and an additional fuel-drop splitting. The fuel drops are split immediately after the fuel nozzle due to the kinetic energy of the rotating high-speed air flow. The particulars of the applied air-assist atomizer can be found in reference [2]. The principal outline sketch of the atomizer is shown in Fig. 2. On the cross section A-A one can see fuel tangential ducts and a fuel swirl chamber. On the cross section B-B the atomizing air path is shown. In our atomizer, the ratio of atomizing air to fuel was in the range from 0.8 to 1.0. A special compressor with pressure ratio of about 2 was provided for the air supply of the atomizer. The inlet of this auxiliary compressor was connected with the outlet of the main compressor. The use of

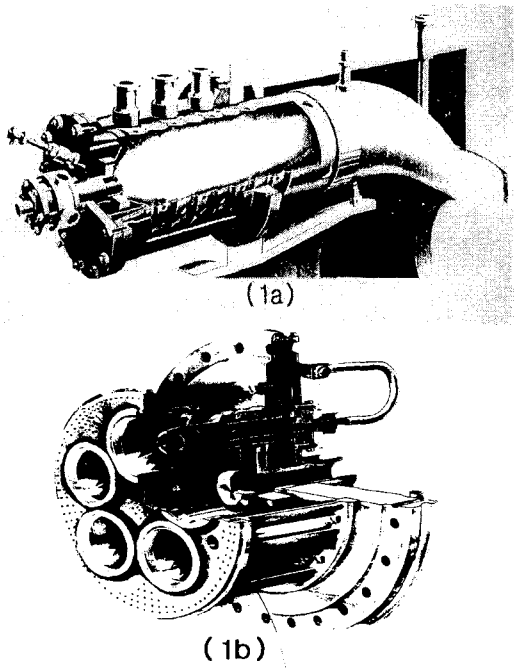

Fig. 1 Combustion chamber of GTE-150:
a. Single-burner combustion section (*first stage of development*);
b. Multi-burner front device.

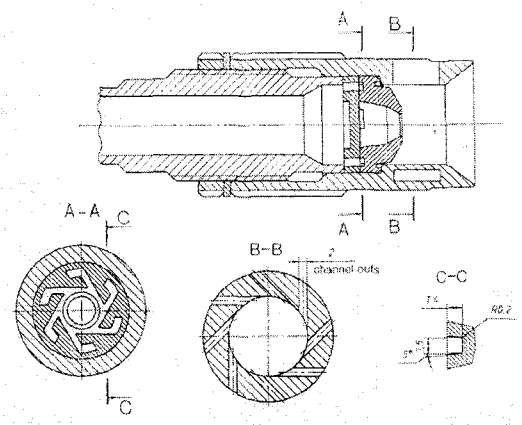

Fig. 2 Air-assist atomizer.

air-assist atomizers has provided a good quality of fuel atomization and acceptable smoke level of the combustion products at the exit of the chimney.

The combustion chamber was equipped with fuel supply and fuel injection systems. Gas turbine

liquid fuel with caloric heat H = 42.530 MJ/kg was used. Every can had its own igniter, which used a propane-air mixture. The subsequent field tests showed that there was no necessity to install all 14 igniters, because the light-round system operated effectively.

The model test program and procedure had the purpose, first of all, to select the best version of the tested combustors, and then to establish the performance characteristics of the combustor: *combustion efficiency, temperature conditions of the* metal, non-uniformity of temperature of gases in front of the turbine (the pattern factor), flame radiation, pressure losses, concentration of harmful emissions in combustion products, etc. The program of field tests repeated the program of model tests, keeping in mind the intention to establish conformity of combustion chamber parameters to the technical design as well as to compare model and field characteristics.

The stand tests were performed on a model section which consisted of a casing, liner, burner device and transition piece. The model section represented one of 14 identical sections of the on-site combustor.

Before beginning the field testing on the power plant, the sections (segments) No. 3 and No. 6 of the on-site combustor were equipped with the necessary devices and indicators for the implementation of the required measurements. In these full-scale sections as well as in the model combustor the necessary measurements were stipulated.

3. RESULTS OF MODEL TESTINGS

The combustion chamber had been ignited reliably. At the moment of ignition, combustion product temperature peak, measured at the exit of the transition piece, had not exceeded 320℃. The character of fuel burning out is shown in Fig. 3 a. Increasing the pressure inside the combustor results in some retardation of burning in the head part of the combustor. At the same time, however, the fuel burning accelerates in the tail part of the liner and compensates its temporary braking in the beginning of the combustion process. In any case the completeness of liquid fuel combustion within the liner length was not less than 99.0 %. The limits of combustion-chamber stability were established by gradual reduction of fuel flow rate till the moment of blowout. The flame blowout took place at an excess-air coefficient α_Σ of more than 17, that corresponds to air heating of less than 130℃. The concentration of oxides of nitrogen (NOx) in combustion products had not exceeded 220 mg/m^3 (hereinafter NOx are given for dry combustion products at O_2=15%).

The temperature condition of the metal is shown in Fig. 3 b. We can see a typical distribution of liner wall temperatures within the length of the separate drums, caused by air film-cooling of the drums and erosion of the jet boundary layer. The temperature maximum is located in the middle of the second drum (counting from the burner towards the transition piece) and amounted to 800 to 820℃. The temperature maximum of the transition piece is located near its exit on a generatrix, inverted to the engine axis. The absolute maximum temperature did not exceed 780℃.

A typical temperature distribution of combustion products at the exit of the transition piece is shown in Fig. 3 c. These data had been received in stand conditions with stationary multidot probes at 30 points. The maximum of the temperature, t_{lT}^{max}, is located at 2/3 of the channels height, starting from the blade root. The relative non-uniformity of the temperature (the pattern factor)

$$100\ (t_{lT}^{max} - t_{lT}) / (t_{lT} - t_A)$$

of 100 % loading was 12 %.

The intensity of the thermal flame radiation J [kW/(m^{2}sr)] was measured in several cross sections of the liner at various modes. The characteristic distribution of π J versus liner length is illustrated in Fig. 4, curves 1 and 2. The maximum of the thermal flame radiation was, in all cases, within the limits of the first two drums and could exceed 500 kW/m^2. The increasing of pressure in the

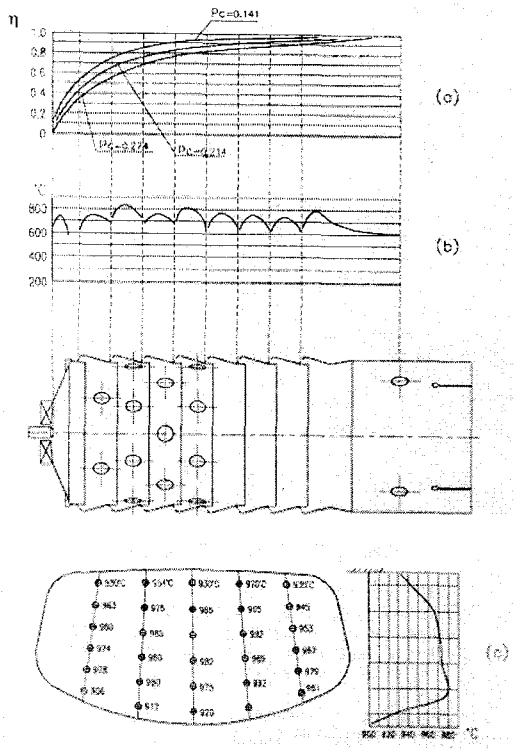

Fig. 3 Results of stand tests; U_S=174.0W/(m^{2}Pa), t_A=370℃, t_{1T}^m=962℃.

a. Combustion efficiency;

b. Liner wall temperature;

c. Distribution of combustion product temperature at the exit of the transition piece.

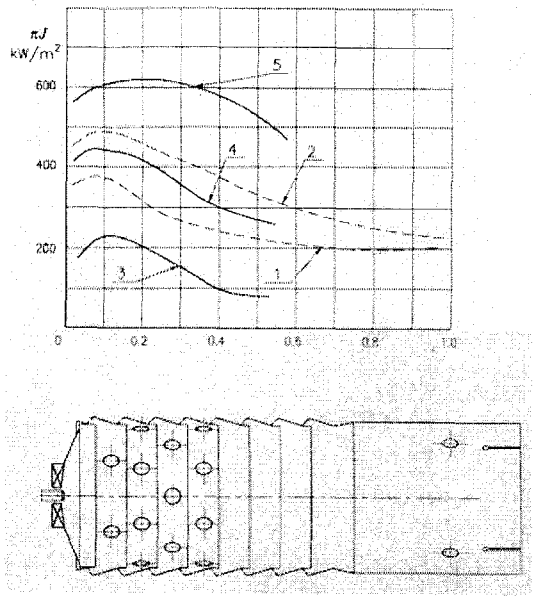

Fig. 4 Thermal flame radiation:

1. Stand tests; U_S=136.0W/(m^{2}Pa), t_A=372℃, t_{1T}^m=950℃, P_C=0.141MPa.
2. Stand tests; U_S=136.0W/(m^{2}Pa), t_A=369℃, t_{1T}^m=950℃, P_C=0.262MPa.
3. Field tests; idle running
4. Field test; N_E=70MW.
5. Field test; N_E=90MW

combustion chamber always resulted in the increasing of thermal flame radiation. We guess the role of soot particles in the flame radiation.

The relative loss of the total (*-top index) pressure 100Δ P*/P_A, measured within the volume of the connecting cylinder exit cross section of the transition piece amounted to 5 %. Practically speaking, in the connecting cylinder, P^*_A=P_A. These data were obtained at an immutable relationship of AT_A/P_A, proportional to air velocity in the liner holes. According to the above-mentioned statements this relationship in the stand tests resulted in (AT_A/P_A) = 40.645 / 1.29 = 20000 kgK/(sMPa). It is completely clear that the non-observance of the specified relationship will result in other aerodynamic characteristics. Note that the rather increased aerodynamic resistance of the combustion chamber under consideration is connected with a severe necessity of a good-quality fuel-air mixing in the flame tube, the combustion loading of which exceeds in more than three times the combustion loading of the former Russian heavy-duty gas turbine GT-100.

The measurements of fluctuating pressure had shown that the instability of burning was absent at all modes; the pressure oscillations appear to be broadband noise with frequencies of 60 to 80 Hz and 80 to 100 Hz. The average peak-to-peak amplitude of fluctuations did not exceed 4 to 5 kPa.

As we have already mentioned, the given results of the stand testing are of concern to the single-burner front device of the combustion chamber. The single-burner device was established

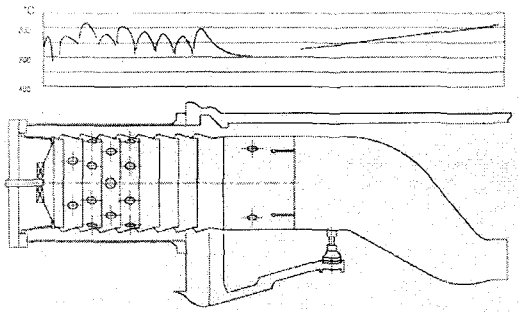

Fig. 5 Field tests, N_E=100MW; liner wall and transition piece temperature

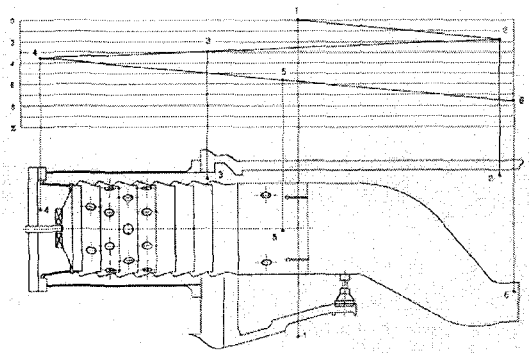

Fig. 6 Field tests, N_E=73.0MW; Pressure loss of air and combustion product.

on the basis of GTE-150 for the first stage of its development. A multi-burner front device, shown in Fig. 1b, was further tested on the test rig. The experiments have shown, that in this case, the burning-out of fuel occurs more intensively and comes to an end on smaller length of the liner. The quality of the combustion chamber from the point of view of maximum metal temperature, the non-uniformity of the combustion product temperature after the transition piece and pressure fluctuations have not worsened. The concentration of nitric oxides has decreased a little. In the stand conditions it has amounted to 200 to 205 mg/m^3. The detailed statement of the stand testing of the multi burner combustor with temperature t_{IT}=1100℃ can be found in the previous paper [1].

4. FIELD TESTS RESULTS: COMPARISON OF MODEL AND FIELD TESTS

It is possible to ascertain a reliable ignition and a reliable light-round of the separate sections. At the moment of ignition, the burst of temperature of gases in front of the turbine (the hurl of the temperature), measured by low-inertia thermocouples, has not exceeded 380℃. At all modes of operation the combustion efficiency has been not less than 99 %. At a loading of 100 MW, the content of nitric oxides in combustion products sampled at the exit of the transition piece has achieved 340 mg/m^3.

The combustion chamber operated quietly and steadily within the whole range of loading. The fluctuating pressure represented a broadband noise with frequencies 60 to 70 Hz and 80 to 100 Hz. The average double (peak-to-peak) amplitude of fluctuations did not exceed 5 to 6 Pa, and this has satisfied the norms, accepted in Russia. At the moment of ignition, at idling and within the whole range of loading, the combustion products smoke emission has not exceeded 3 to 4 SAE smoke number. At the chimney exit of the GTE-150, a slightly grayish smoke appeared contrasting with smoke of the neighboring chimney exit of GT-100. The moderate smoke emission of the GTE-150 exhaust gas was a consequence of application of the air-assist atomizers.

Enough items of information have been obtained concerning the liner wall temperature within the wide range of loading. In Fig. 5, the characteristic distribution of wall temperature versus liner length can be seen. It is similar to liner wall temperature distribution of the model combustion chamber. Within the limits of every drum the maximum temperature is located on its middle. At the drum edges a rather low temperature is found. Such a distribution was caused by film cooling of the drum surface oriented to the flame. The maximum liner wall temperature of 830℃ was found on the second drum. It was 20 to 30℃ higher than maximum liner wall temperature of the model

combustor under the same operating conditions. Also, Fig. 5 illustrates the temperature of the liner and transition piece. We notice that the maximum transition piece temperature of 820℃ was located in its exit cross section on a generatrix, inverted to the axis of the turbine. Similar result was obtained with the model testing, however the maximum temperature of the model combustor was lower by about 30℃.

In an earlier published paper [3] a rather significant role was found for the pressure in a combustor P_C on the flame emissivity ε_F and effective temperature of the flame radiation T_F. The present comparative research of model and full-scale combustors has confirmed the essential influence of P_C on ε_F and T_F . Really, the flame radiation intensity J, measured within a zone of active fuel burning considerably exceeds the appropriate value of J measured in the model combustor as shown in Fig. 4. This circumstance is connected with the increase of the flame emissivity ε_F and the effective temperature of the flame radiation T_F at the transition from stand tests to field tests, since $P_C^N > P_C^M$. The value of ε_F increases because of the increase of media optical density; T_F increases because of the increase of the number of fuel-rich, high-temperature pockets. In these pockets the local temperature is close to the temperature $T_{\alpha=1}$ that is equal to the adiabatic flame temperature at the stoichiometric fuel / air ratio.

Pressure measurements were made in a number of points within the air and combustion products path. Thus, the absolute and relative pressure loss of the actual combustor as well as its elements were determined. Fig. 6 shows the disposition of measuring points. At points 1 and 6 the measurements have been performed by total pressure probes (i.e. P_1^* and P_6^* have been measured), and at points 2, 3, 4, and 5 the static pressures P_2, P_3, P_4, and P_5 have been measured. The corrections on a dynamic pressure here were made.

It was found that the relative pressure loss of the total site mentioned, i.e. $100(P_1^*-P_6^*)/P_1^*$ or its

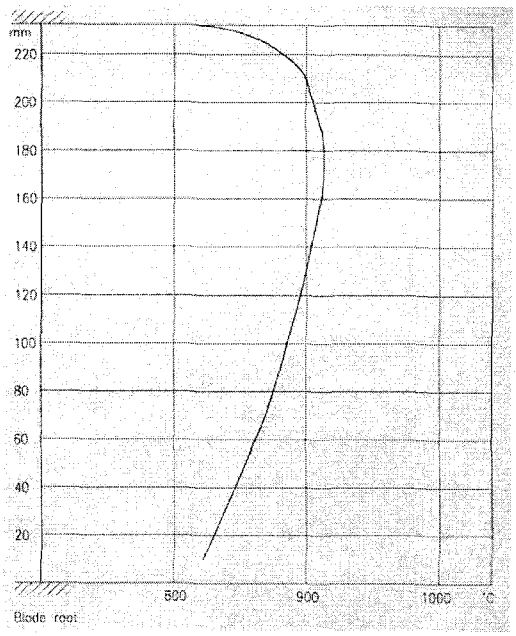

Fig. 7 Field tests, N_E=41.0MW; radial distribution of combustion product temperature at the turbine entrance

separate sites $100(P_1^*-P_1^*)/P_1^*$, practically did not depend on loading. For the designed single-burner combustion section, on the average, $100(P_1^*-P_6^*)/P_1^* = 7.49$ %. There are two reasons for the larger pressure loss in the full-scale combustion chamber in comparison with the model. *Firstly, in the conditions of the full-scale combustor* the value of relationship AT_A/P_A is other than it should be from the design parameters of air on the combustor entrance. Really, in field-tests the relationship mentioned was not less than 2100 kgK/(sMPa). Secondly, at the stand conditions the pressure in the point 1 (see Fig. 6) i.e. at the exit of air from the axial compressor was not measured. Therefore only the pressure loss in the actual combustion chamber i.e. $100(P_2^*-P_6^*)/P_2^*$ was determined which, naturally, was less than $100(P_1^*-P_6^*)/P_1^*$.

The analysis of the data received concerning the pressure loss shows also that about one quarter of the total pressure loss was in the transition piece. The over estimated pressure loss was caused, in

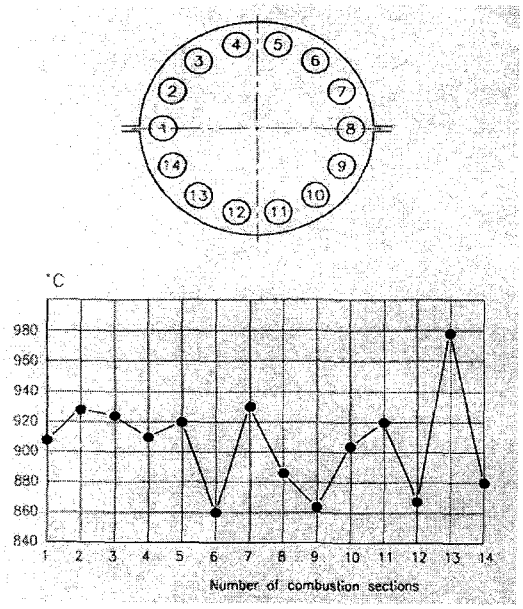

Fig. 8 Field tests, N_E=90.0MW; circle distribution of the combustion product temperature at the turbine entrance

particular, by the non-uniform speed and non-uniform temperature of combustion products at the entrance of the transition piece. Keeping in mind the amendment on the relationship AT_A/P_A , the pressure losses within the sites 2-5 of model and full-scale combustors were identical.

A typical combustion product temperature distribution in the radial direction, obtained by a traversing probe near the exit of the transition piece can be seen in Fig. 7. The maximum temperature was located at 2/3 of the channel height, measured from the blade root. The identical radial distribution of temperature t1T had been obtained in the model testing. Irrespective of loading of the gas turbine it was found that

$$100\ (t_l^{max} - t_{lT}) / (t_{lT} - t_A) = 8.8 \text{ to } 12.0\ \%.$$

This was recognized as a satisfactory characteristic. The value of this characteristic have been coincided with similar one obtained earlier with model testing.

A circuit gas temperature non-uniformity at the gas turbine entrance (the pattern factor) is by no means the important gas turbine characteristic. With our model testing, this kind of characteristic could not be obtained. It is completely clear, that the circuit non-uniformity of the gas temperature is determined by the non-uniformity of the fuel and air distribution among separate sections of the combustion chamber. The experience and theory convince us that the fuel distribution is more difficult than the air distribution, because of the different height location of atomizers and because of very small through passage areas of its fuel channels. The leading gas turbine firms have overcome these difficulties by the installation of volumetric fuel batchers, which distribute the fuel among the sections independent of the difference in the height location of atomizers and through passage areas of fuel channels. The fuel batchers were not installed on the GTE-150. The uniformity of fuel distribution was achieved by a selection of atomizers with various flow rate characteristics.

The circuit gas temperature non-uniformity at the turbine entrance has been obtained by measurement of combustion product temperatures with low-inertia thermocouples. In every transition piece the thermocouple was located at 2/3 of the channel height measured from the blade root. This temperature was designated as $t_{C.P.}$ A typical distribution of circuit temperatures is shown in Fig. 8. We can ascertain that the temperature distribution is not uniform. We use for the description of the circuit non-uniformity of the temperature the same characteristics as for the description of the above considered radial non-uniformity. We define $t_{C.P}^{Max}$ as the value of maximal temperature measured, and $t_{C.P}^{m}$ as the mass mean temperature of combustion products at the turbine entrance. According to the measurements and calculations, the difference of temperatures $(t_{C.P}^{Max} - t_{C.P}^{m})$ in the range of loading of 60 to 90 MW amounts 90℃, having a weak tendency to increase in the process of loading growth. The characteristic

$$100\ (t_{C.P}^{Max} - t_{C.P}^{m}) / (t_{C.P}^{m} - t_A)$$

was equal to 10 to 15 % and did not appear to have a predictable travel in the process of loading growth.

5. CONCLUSION

The model testing and improvement of the combustion chamber with observance of the above mentioned test procedures allows an objective judgement to be made about the basic characteristics of the on-site combustion chamber: stability and completeness of fuel combustion, smoke emission, pressure loss, radial non-uniformity of gas temperature at the turbine entrance, NOx emissions, and temperature situation of the metal.

The stability and combustion efficiency of the on-site combustion chamber have not been lower than those in the model combustion chamber.

The application of air-assist atomizers has beneficently affected the combustion efficiency, pattern factor, liner wall temperature and smoke emission. In the model and on-site combustors smoke emission has not exceeded the 4 SAE smoke number.

The relative aerodynamic pressure loss in similar locations of model and on-site combustors have been identical.

The position of the gas temperature maximum t_{lT}^{max} in the radial direction in model and on-site combustors has been identical.

The characteristic of the radial non-uniformity of the gas temperature at the turbine entrance

$$100\ (t_{lT}^{max} - t_{lT}^{m}) / (t_{lT}^{m} - t_A)$$

in the on-site combustor has been higher by 2 to 3 % than in the model combustor. This circumstance is explained by a delayed burning in the on-site combustor in which the pressure was much higher as compared to the model conditions.

The thermal flame radiation in the on-site combustor was found to be higher than in the model combustor in accordance with calculation of ε_F and T_F [3].

Emissions of nitric oxides in the on-site combustor were higher than in the model combustor. When using the well known and accepted relationship

$$(NOx)^N = (NOx)^M (P_C^N / P_C^M)^n,$$

where the exponent n is a constant, we have obtained n = 0.30. The lower value of the exponent n, in comparison with the known value of n = 0.50, has been caused by rather intensive mixing of fuel and air in the combustion chamber of GTE 150 studied here. Here the air velocity in the combustion holes amount to 70 to 90 m/s.

In the model and on-site combustors, the fluctuating pressure represented a broadband noise with frequencies 60 to 70 Hz and 80 to 100 Hz. The average peak-to-peak amplitude of fluctuations did not exceed 5 to 6 Pa and that has satisfied the norms accepted in Russia.

The position of maximum liner wall temperature as well as the character of distribution of temperature on its length are identical in both combustors. The position of maximum liner wall temperature was on the middle of the second drum, counting from the burner. The value of the liner wall and the transition piece temperature in the on-site combustor was higher by 20 to 30℃ as compared to the model combustor.

REFERENCES

1. V. Antonovsky, V. Akoulov, V.Shvedkov, Some results of stand testing of the GTE-150 combustor at mean mass gas temperature at the turbine entrance 1100℃, CKTI Papers, vol. 261, pp. 151-156, Leningrad, 1990.
2. V. Antonovsky, V. Akoulov, V. Shvedkov, O. Lesnjak. Stand investigation of GTE 150 at application of air-assist and airblast atomizers, CKTI Papers, vol. 266, pp. 49-56, Leningrad, 1991.
3. Antonovsky V. I. Thermal Radiation of Flame in Gas Turbine Combustion-chambers Experiment and Calculation. PROCEEDINGS OF THE THIRD INTERNATIONAL SYMPOSIUM ON EXPERIMENTAL AND COMPUTATIONAL AEROTHERMODYNAMICS OF INTERNAL FLOWS, September 1 6, 1996. World Publishing Corporation, p.970 - 972.